A porphycene-gentamicin conjugate for enhanced photodynamic inactivation of bacteria

A porphycene-gentamicin conjugate for enhanced photodynamic inactivation of bacteria

Ingrid Nieves,[a] Cormac Hally,[a,b] Cristiano Viappiani,[b] Montserrat Agut[a] and Santi Nonell*[,a]

[a] Institut Químic de Sarrià, Universitat Ramon Llull, Via Augusta 390, 08017, Barcelona, Spain

[b] Dipartamento di Scienze Matematiche, Fisiche e Informatiche, Università di Parma, Parco Area delle Scienze 7A, 43124, Parma, Italy

* Corresponding author: santi.nonell@iqs.url.edu

Abstract

A novel photoantimicrobial agent, namely 2-aminothiazolo[4,5-*c*]-2,7,12,17-tetrakis(methoxyethyl)porphycene (ATAZTMPo-gentamicin), conjugate has been prepared by a click reaction between the red-light absorbing 9-isothiocyanate-2,7,12,17-tetrakis(methoxyethyl)porphycene (9-ITMPo) and the antibiotic gentamicin. The conjugate exhibits submicromolar activity *in vitro* against both Gram-positive and Gram-negative bacteria (*Staphylococcus aureus* and *Escherichia coli*, respectively) upon exposure to red light and is devoid of any cytotoxicity in the dark. The conjugate outperforms the two components delivered separately, which may be used to enhance the therapeutic index of gentamicin, broaden the spectrum of pathogens against which it is effective and reduce its side effects. Additionally, we report a novel straightforward synthesis of 2,7,12,17-tetrakis(methoxyethyl) porphycene (TMPo) that decreases the number of steps from nine to six.

Keywords: antimicrobial resistance; photodynamic therapy; porphycene; singlet oxygen; photosensitizer conjugates; amphiphilicity.

1. Introduction

Antimicrobial resistance (AMR) is an increasingly serious threat to the gains made in health and development.[1] It has been estimated that in the EU in 2015 about 33,000 people died from infectious diseases caused by multidrug-resistant bacteria.[2] Current antibiotics are often insufficiently because of AMR, so, alternative anti-infective approaches are urgently needed and do not cause resistance themselves. Antimicrobial photodynamic therapy (aPDT) is a potential alternative treatment that is currently gaining a lot of attention due to its broad spectrum of action, its multitarget mechanism of action, its efficiency against antibiotic-resistant strains, and its very low potential for eliciting resistance by itself.[3] aPDT is a local treatment based on the generation of reactive oxygen species (ROS), particularly singlet oxygen ($^1O_2$),[4,5] upon exposure of a photoantimicrobial drug, referred to as the photosensitizer (PS), to light of a suitable wavelength. In the presence of oxygen, $^1O_2$ or other ROS are generated and cause oxidative damage to a large number of cell components, leading to cell death. Damage to the host tissue is minimized by exposing the lesion to light very soon after PS delivery, before it can be uptaken by the host tissue.[6] Although aPDT is effective against both Gram-positive and Gram-negative microorganisms, photoinactivation of the latter requires, in general, the use of chemical agents to permeabilise their more complex outer wall, e.g., Tris/EDTA or polycationic agents, as well as cationic PSs that bind to the negatively-charged residues on the outer wall.[7,8]

Among the PSs being currently scrutinized for aPDT applications, porphycenes stand out as excellent candidates owing to their broad and strong absorption and fluorescence in the red/near-IR spectral region, where tissue is most permeable to light (600–900 nm), and to a high $^1O_2$ photoproduction efficiency.[3] Porphycenes have been mostly applied to photodynamic therapy of cancer and only recently have begun to be explored for aPDT applications.[4] In the cancer field, Richert and co-workers described that 2,7,12,17-tetrakis(methoxyethyl)porphycene (TMPo), showed excellent fluorescence and photosenzitising properties, adequate solubility in biological media, efficient uptake by cancer cells, and very promising photodynamic activity in mice assays.[10] Nevertheless, antimicrobial photoinactivation studies performed with TMPo revealed the limitations imposed by a lack of hydrophilicity and positive charges, thus requiring either solubilization agents such as Pluronic

F-127[11] or coupling of the porphycene core with cationic polylysine moieties[12,13] for effective delivery to bacteria.

A current trend to tackle multi-drug resistant bacterial infections is to administer a combination of antibiotics[14] that target different cellular components. From this perspective, the combination of aPDT with antibiotics seems ideally suited to overcome the majority of resistance mechanisms owing to the multitarget nature of aPDT, and has the added benefit that those bacteria that might survive the photodynamic insult will still be exposed to the antibiotic, precluding their regrowth.[15] Early studies combining aPDT with antibiotics have observed promising effects ranging from additive to synergistic.[16–20] Of particular interest is the approach by Cahan et al. who have linked covalently the PS Rose Bengal to the antibiotics 6-aminopenicillanic acid and kanamycin.[16] We pursued a similar approach linking antimicrobial peptides to a porphycene and a series of porphyrins.[21,22]

In this work, we have linked the aminoglycoside antibiotic gentamicin to the porphycene TMPo. Gentamicin is a well-established antibiotic, effective against Gram-negative bacteria but with limited activity against Gram-positive microorganisms. However, many bacteria have developed resistance to this antibiotic[23] and there is still no selective method for combating this resistance nor the nephrotoxic and ototoxic side effects.[24] Since gentamicin contains residues that will be protonated at physiological pH, conjugation of gentamicin to TMPo is expected to enhance the pharmacological and photoantimicrobial activity of TMPo due to a higher aqueous solubility and higher affinity for the negatively-charged outer cell wall of Gram-negative bacteria..[25] On the other hand, conjugation may also lead to a reduction in the amount of gentamicin required for treating pathogenic bacterial infections and hence its side effects in adults.[24]

Herein, we present a new straightforward synthetic route for the TMPo scaffold, the synthesis and photophysical characterisation of the novel ATAZTMPo-gentamicin conjugate, and we explore its potential as a photoantimicrobial agent for the photoinactivation of Gram-positive and Gram-negative bacteria.

2. Results

2.1 Synthesis

Synthesis of TMPo

The synthesis of TMPo was first reported by Vogel and co-workers, requiring nine synthetic steps.[10,26] This classical approach consisted in the formation of a *β*-pyrrole by means of Fischer methodology or Knorr condensation, followed by two coupling reactions, namely an Ullmann coupling, which afforded the 2,2'-bipyrrole moiety, and a subsequent McMurry coupling. Nevertheless, Vogel's route and other recent alternative approaches[27,28] for the preparation of porphycenes are associated with harsh reaction conditions, poor regioselectivity, poor yields, and a large number of steps.

As part of our continuous efforts to simplify the synthesis of porphycenes, this work describes a novel three-step synthetic strategy for the preparation of gram quantities of *β,β*– alkoxyalkyl-2,2'-bipyrroles and apply it to the synthesis of TMPo, decreasing from nine to six the number of steps required.

The synthesis of the *β,β*-alkoxyalkyl-2,2'-bipyrrole **4** (Figure 1) was an extension of our previously reported one-pot access to *β,β'*–aryl 2,2'-bipyrroles,[29] by a tandem reaction based on the oxidative dimerization of a 2-(trimethylstannyl) pyrrole generated *in situ* by a van Leusen-type methodology, which is unprecedented in the literature for alkoxyalkyl substituents. For this purpose, the commercially available 3-methoxypropanol **1** was chosen as starting material. Gratifyingly, oxidation of **1** in the presence of the mild oxidant 2-iodoxybenzoic acid (IBX)[30] led to the corresponding aldehyde **2** in excellent yield (85%), in contrast to other common oxidants reported in literature, such as pyridinium chlorochromate (37%).[31] The aldehyde **2** was then elongated by Horner-Wadsworth-Emmons (HWE) olefination to give the *α,β*-unsaturated ester **3** as a mixture of isomers (*E:Z*; 98:2). The stereochemical assignment of the new double bond was made by comparison of the coupling constants. Then, ethyl 5-methoxypent-2-enoate **3** was subjected to the pyrrole [3+2] ring-forming process, in the presence of tosylmethyl isocyanide (TosMIC) and trimethyltin chloride under basic conditions, leading to the intermediate 2-(trimethylstannyl)pyrrole. Subsequent addition of copper (II) nitrate afforded the desired 2,2'-bipyrrole **4** in a poor yield. The reaction yield could be improved by

fine tuning the reaction stoichiometry. Specifically, optimum yields were obtained when TosMIC was increased from 1 to 1.5 equiv., and copper (II) nitrate was added stepwise (1 equiv. per 40 min). Under those conditions, the first 4,4'-alkoxyalkyl functionalised 2,2'-bipyrrole **4** was obtained in 25% yield, which is in excellent agreement with those described for alkoxyaryl bipyrroles (25% for 4-methoxy- and 27% for 3,5-dimethoxy bipyrroles).[29]

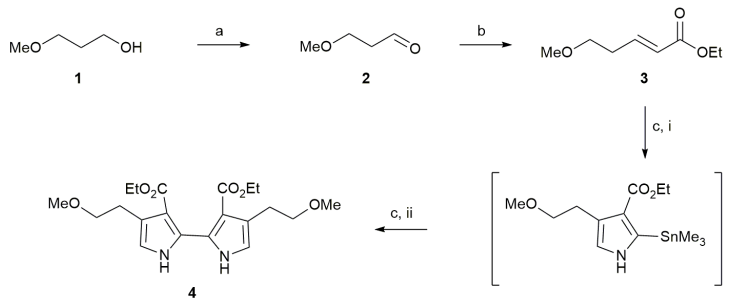

Figure 1 Synthesis of 2,2'bipyrrole **4**. Reagents and conditions: (a) IBX, EtOAc, refluxed, 12h, 85%; (b) Triethyl phosphonoacetate, NaH, THF, 0 ºC, 2 h, 75% (*E:Z*;98:2); (c) i) TosMIC, BuLi, Me_3SnCl, THF, -78 ºC to RT, 2 h; ii) $Cu(NO_3)_2 \cdot 3H_2O$; RT, 2 h, 25%.

With 2,2'-bipyrrole **4** in hand, we examined the stability of the methoxyethyl group under a direct saponification and decarboxylation reaction (Figure 2). Thus, the use of sodium hydroxide in ethylene glycol[32] provided successfully the α-free bipyrrole **5** in just one step, which was subjected to next reaction without further purification due to its tendency to polymerise. Finally, conventional Vilsmeier-Haack formylation, followed by McMurry reductive cyclisation afforded the porphycene TMPo in 25% yield, which reproduces that reported by Richert *et al.*[10]

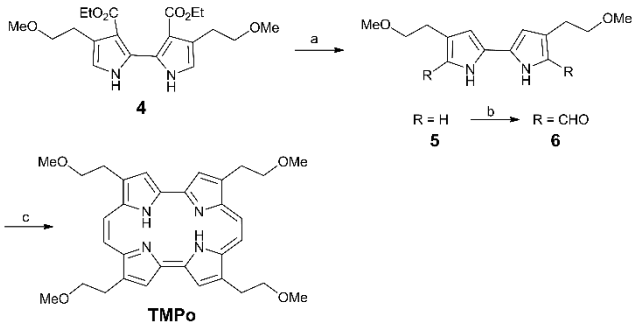

Figure 2 Synthesis of TMPo. Reagents and conditions: (a) NaOH, ethylene glycol, 180 ºC, 1.5 h, 85%; (b) i) $POCl_3$, DMF, 60 ºC, 1 h; ii) NaOAc, H_2O, 85 ºC, 1 h, 80%; (c) i) $TiCl_4$, Zn, Cu_2Cl_2, THF, refluxed, 5 h; ii) K_2CO_3, H_2O, 0 ºC to RT, 1 h, 25%.

Synthesis of ATAZTMPo-gentamicin conjugate

TMPo has been functionalised at 9-position with an isothiocyanate group (9-ITMPo). 9-Isothiocyanateporphycenes undergo a click reaction with amino-substituted compounds yielding a thiourea that spontaneously evolves to a near-IR absorbing 2-aminothiazolo[4,5-*c*]porphycene (ATAZPo).[33,34] We hypothesized that this would be the case also when 9-ITMPo would be allowed to react with the less-hindered primary amino-group of gentamicin, enabling conjugation through a one-step reaction.

As depicted in Figure 3, the synthesis of 9-ITMPo was envisaged by using the methodology developed by Vogel and co-workers, consisting in a mono-nitration of TMPo at the *meso* position (9-NTMPo) and subsequent Zinin reduction of the nitro group to the amine (9-ATMPo).[35] The resulting 9-ATMPo was subjected to 1,1′-thiocarbonyldi-2(1*H*)-pyridone[33] in DCM, which afforded the corresponding 9-ITMPo in 80% yield over three-steps.

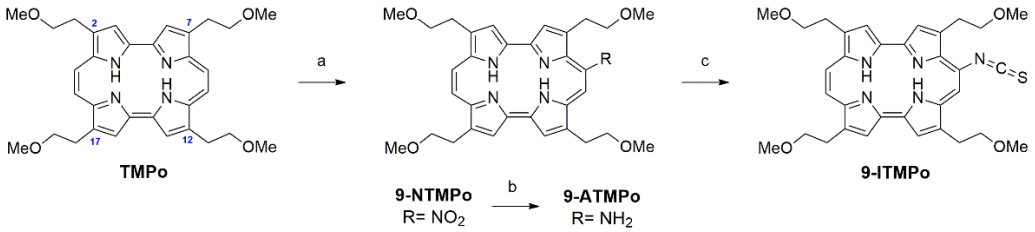

Figure 3 Synthesis of 9-ITMPo. Reagents and conditions: (a) $AgNO_3$, acetic acid glacial : DCM (10:7), 55 ºC, 20 min, 100%; (b) NaOH, $Na_2S_2O_4$, DMC, reflux, 1 h, 95%; (c) 1,1′-thiocarbonyldi-2(1*H*)-pyridone, DCM, RT, 16 h, 80%.

Gentamicin sulphate is a mixture of several congeners, in which gentamicin C1, C1a, and C2 are the three major components of the complex (Figure 4, A). Despite all these distinct forms, we aimed to single couple the less hindered primary C6'-amino group of gentamicin's purpurosamine moiety with 9-ITMPo, in order to alter as little as possible the pharmacokinetic properties of the antibiotic.[36] For this purpose, a high molar excess of the aminoglycoside was added to the reaction mixture, and basic pH was adjusted with potassium carbonate powder to ensure the basic state of the primary amino-groups.[37] The reaction conversion could be monitored visually due to the distinct colour progression that the 18π-electron system of 9-ITMPo (dark-green) suffers when it transformed into the

corresponding thiourea-intermediate (dark-blue) and it subsequently evolved to the 22π aromatic thiazolo-conjugate ATAZTMPo-gentamicin (light green) (Figure 4, B).

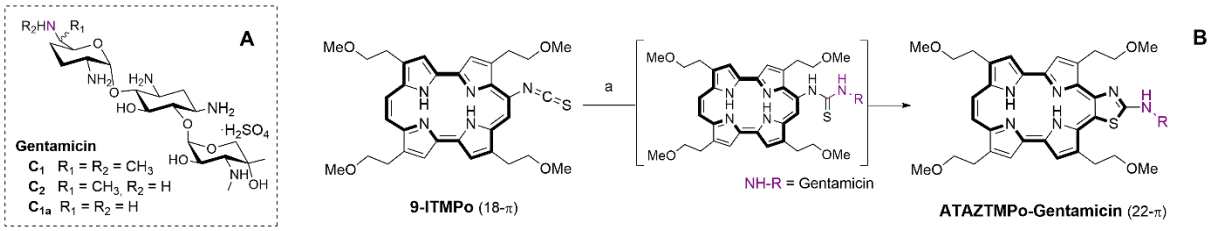

Figure 4 [A] Chemical structures of gentamicin C_1, C_{1a}, and C_2; **[B]** Click reaction-mediated conjugation of antibiotic gentamicin. Reagents and conditions: (a) gentamicin, K_2CO_3, ethanol absolute, RT, 5 days, 80%.

The mono-conjugated ATAZTMPo-gentamicin was then purified from the antibiotic excess, and from undesired porphycene by-products, by flash column chromatography on C18-reversed phase (RP) silica-gel (see Experimental Section for details). Subsequent RP-HPLC analytical characterisation of the pure fraction was challenging since retention of the conjugate in RP-HPLC was largely observed due to its intrinsic amphiphilic character. Gratifyingly, after carefully tuning the elution conditions, the desired compound was detected showing a chromatographic profile similar to those reported by Woiwode *et al.* for gentamicin-Texas red probe as a mixture of species of the aminoglycoside (Figure S1 and S2).[37] Finally, the *m/z* mass values of the eluted peaks at retention time around 3.4 min confirmed the single-conjugate for the most abundant charge state of $z = 1$ and $z = 2$.[37,38]

2.2 Photophysical characterisation

The photophysical properties of 9-ITMPo and ATAZTMPo-gentamicin in methanol are summarised in Table 1. As depicted in Figure 5, the absorption spectra of 9-ITMPo and ATAZTMPo-gentamicin show the characteristic Soret and Q bands of asymmetric porphycenes in methanol.[39] Additionally, the cyclised conjugate is endowed with red-shifted absorption and fluorescence spectra in comparison with its 18-π precursor as a result of the expanded 22-π electronic delocalisation system. The observed spectral changes of ATAZTMPo-gentamicin correlate with the results described by Planas and co-

workers for fused tetraphenylporphycenes,[33] in which absorbance of the compounds shifted to the near-IR, where tissues are most transparent to light and present less autofluorescence.[40]

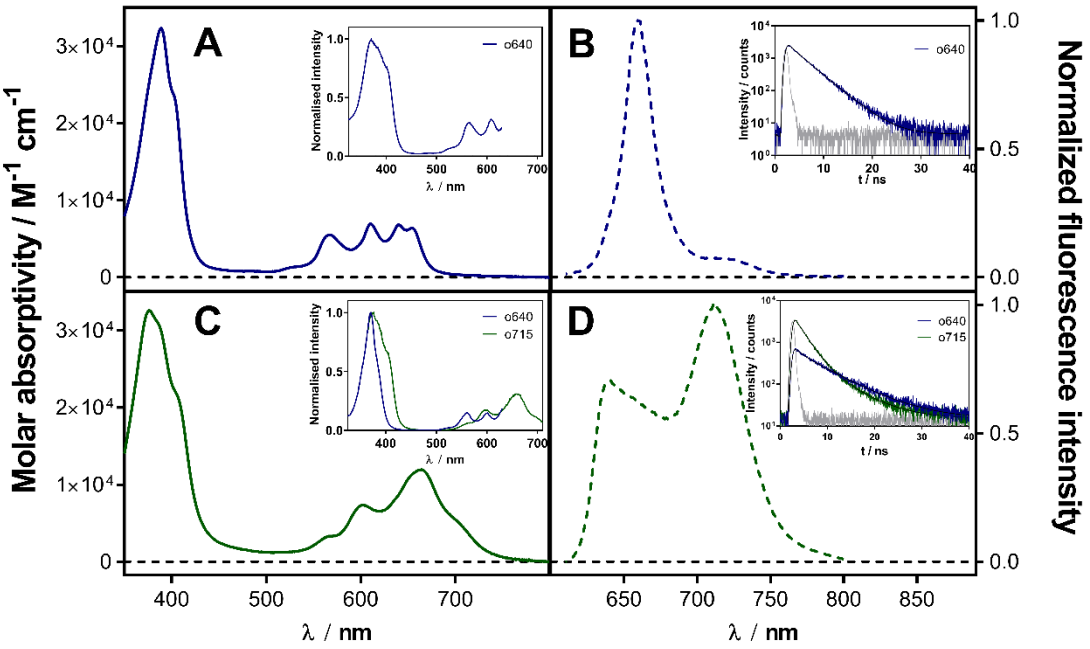

Figure 5 (A,C) Absorption and (B,D) fluorescence spectra of 9-ITMPo (A,B) and ATAZTMPo-gentamicin (C,D) in methanol respectively. Insets: (A,C) Excitation spectra of the fluorescence observing at 640 and 715 nm when indicated. (B,D) Time-resolved fluorescence of either compound exciting at 596 nm. Signal, fit and instrument response function (IRF) at 640 and 715 nm (λ_{exc}= 596 nm).

In sharp contrast, the fluorescence spectrum of the conjugate exhibits two emission bands compared to the single emission of the precursor 9-ITMPo. Further details were obtained from time-resolved fluorescence analysis. While 9-ITMPo fluorescence decays with monoexponential kinetics (τ_s = 3.4 ns; Table 1), ATAZTMPo-gentamicin decays with a biexponential kinetics indicating two different populations of the excited singlet state of the PS. The fluorescence decay kinetics presented one major component (73%, 22-π electron system) which decays much faster, τ_1 = 1.9 ns, in contrast to the minor excited-state specie with lifetime τ_2 = 6.1 ns (27%, 18-π electron system). These values were obtained by deconvolution of the spectrum of time resolved emission spectra (Figure S3). Laser flash photolysis determined triplet lifetimes of either compounds to be in tens of microseconds range in argon-saturated methanol (Figure S4).

Table 1 Summary of optical and photophysical properties of 9-ITMPo and ATAZTMPo-gentamicin in MeOH

Compound	λ_{max} [a]/ nm	ε [b]/ $M^{-1}cm^{-1}$	λ_F [c]/ nm	Φ_F [d]	τ_s [e]/ ns	τ_T [f]/ µs	Φ_Δ [g]
9-ITMPo	640	6.8 x 10^3	659	0.26	3.4	74	0.59
ATAZTMPo-gentamicin	664	1.2 x 10^4	643, 713	0.10	τ_1 = 1.9 (73 %) τ_2 = 6.1 (27%)	66	0.29

[a] Maximum absorption wavelength at the Q-region. [b] Molar extinction coefficient at λ_{max}. [c] Wavelength of fluorescence. [d] Fluorescence quantum yield, *meso*-tetraphenylporphyrin as reference (Φ_F (toluene) = 0.11).[41] [e] Singlet state lifetime in air-saturated methanol, (amplitudes). [f] Triplet state lifetime in argon saturated methanol (µs) obtained by transient absorption spectroscopy. [g] Singlet oxygen quantum yield, phenalenone as reference (Φ_Δ (MeOH) = 0.97).[42]

A unique feature of thiazoloporphycenes is the existence of an equilibrium between 18π and 22π electronic systems, whereby the 18π form is stabilized in strong hydrogen-bond donating (HBD) solvents, while the 22π system is favoured in weaker- or non-HBD solvents. [34] In this regard, the absorbance and the fluorescence of ATAZTMPo-gentamicin were measured in three solvents of different HBD capacity, such as phosphate-buffered saline (PBS; pH 7.4), methanol (MeOH), and dimethyl sulfoxide (DMSO). As shown in Figure 6, the absorption spectra in PBS loses much of its structure and exhibits lower molar absorption coefficients, which is consistent with the aggregation that several porphyrin-like compounds tend to experience in aqueous media. The absorbance spectrum suffers a hypochromic shift in comparison with organic solvents and its bands are less structured and broader. Moreover, the fluorescence spectra in PBS shows a single emission band at λ = 640 nm, typical of the 18-π electronic system. Consistent with this, the fluorescence excitation spectrum (Figure S5) indicates that the emission originates from a monomeric species with 18-π electronic system, as observed previously for a related porphycene.[8] A gradual conversion to the near-IR absorbing species is observed when non-aqueous and weaker- (MeOH) or non-HBD (DMSO) solvents are used. Thus, the ATAZTMPo-gentamicin conjugate presents a major near-infrared emission band at approximately λ = 720 nm in DMSO, corresponding to the 22-π expanded electronic system, while in MeOH it shows an intermediate behaviour, which is in concordance with the previously reported for tetraphenyl analogues.[34] To further support this interpretation, compound 2-*N*-butylaminothiazolo-

[4,5-c]-tetrakis-2,7,12,17-(methoxyethyl)porphycene (ATAZTMPo-butylamine, see ESI for details) was also studied since it is the PS's analogue without the antibiotic moiety. It also shows a dual emission in methanol. The ratio of the short-to-long wavelength bands is smaller than for the gentamicin conjugate but is also strongly solvent dependence: it increases in hexafluoro-2-propanol (HFIP, a strong HBD solvent) and decreases in DMSO (see Figure S6 in the supplementary information), following the same trend as that observed for the gentamicin conjugate. This confirms that the ratio of the two emissions reflects the equilibrium between the 18π and 22π electronic systems, and suggests that gentamicin stabilizes the zwitterionic 18π system, likely by forming hydrogen bonds through its free amino groups.

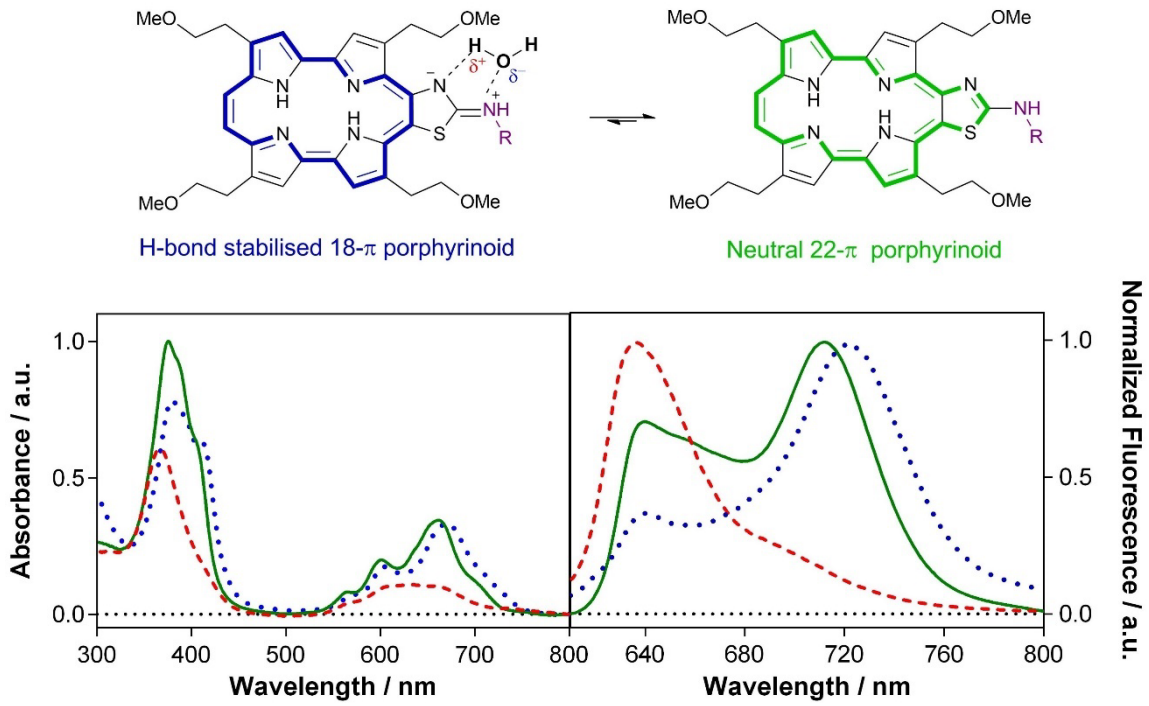

Figure 6 Top: Equilibrium between the 18-π and 22-π forms of ATAZTMPo-gentamicin. Bottom: Absorbance (left panel) and normalised fluorescence emission spectra (right panel) of ATAZTMPo-gentamicin (8 μM) in MeOH (full green line), DMSO (dotted blue line) and PBS (dashed red line).

The ability ATAZTMPo-gentamicin to sensitise the production of $^1O_2$ was studied by direct observation of its phosphorescence at 1275 nm in methanol, heavy water and dimethyl sulfoxide. Table 2 collects the values of the singlet oxygen quantum yield (Φ_Δ) measured (Figure S7).

Table 2 Singlet oxygen quantum yields of ATAZTMPo-gentamicin in air-saturated methanol, heavy water and dimethyl sulfoxide.

Solvent	D_2O[a]	CH_3OH[b]	$(CH_3)_2SO$[c]
Φ_Δ	0.02	0.29	0.36

[a] PNS was used as reference (Φ_Δ =1.03)[43]; [b] PN used as reference (Φ_Δ=0.97)[42]; [c] Fullerene C_{60} used as reference (Φ_Δ=1)[44].

The Φ_Δ of ATAZTMPo-gentamicin presents different efficiencies depending on the polarity and the H-bond donor properties of the solvent in which the conjugate is dissolved. To begin, the Φ_Δ in heavy water is very low (Φ_Δ = 0.02) in comparison with the values in organic solvents mainly due to the aggregation of the compound. The slight differences in Φ_Δ in the two organic solvents can be due to the stabilization of different proportions of the two electronic systems (18π and 22π) caused by the different polarity and HBD strength of the solvents. If these species have different Φ_Δ, the overall yield of the compound would reflect this equilibrium in its overall (and measurable) quantum yield. Up to date it has not been possible to elucidate the individual Φ_Δ values.

For comparison, the Φ_Δ value of ATAZTMPo-butylamine in methanol was also measured and found higher (0.46) than that of the gentamicin conjugate (0.29) (Figure S8). This considerable difference in quantum yields may be due to photoinduced electron transfer (PET) quenching of the thiazoloporphycene excited states by gentamicin, a common observation in porphyrinoids substituted with moieties containing amino groups.[45,46] The amino group directly attached to thiazoloporphycene ring is unlikely to participate in the PET process due to the delocalization of its electron pair across the macrocycle, hence PET quenching is not expected in the butylamine derivative.

2.3 Photoinactivation studies

To assess the potential of the ATAZTMPo-gentamicin conjugate as a novel photoantimicrobial agent, tests against representative members of Gram-positive (*Staphylococcus aureus*) and Gram-negative (*Escherichia coli*) bacteria were performed. Taking into consideration the survival fraction of both strains when they were dark-incubated with different gentamicin concentrations upon experimental

conditions (see Figure S9), the photoinactivation of ATAZTMPo-gentamicin was first attempted in *E. coli* at 8 μM (3.8 μg mL^{-1}) and 45 $J \cdot cm^{-2}$ light fluence (Figure 7). Additionally, ATAZTMPo-butylamine was tested under the same conditions either alone or combined with gentamicin, but not covalently bound. Surprisingly, only the conjugate ATAZTMPo-gentamicin was able to completely eliminate the strain without showing any dark toxicity, whereas the PS and the antibiotic alone failed to effectively inactivate the bacteria. The concentration used (8 μM, 3.8 μg/ml) is close to the reported minimum inhibitory concentration (MIC; 4 μg/ml).[47] However, MIC values are determined at inoculum sizes (CFUs/mL) 100-1000-fold more diluted than those used in this work and, in addition, the antimicrobial effect is measured after incubating the drug for 24 h, while only 1-h contact was allowed in our experiments. Therefore, the lack of dark toxicity is not surprising.

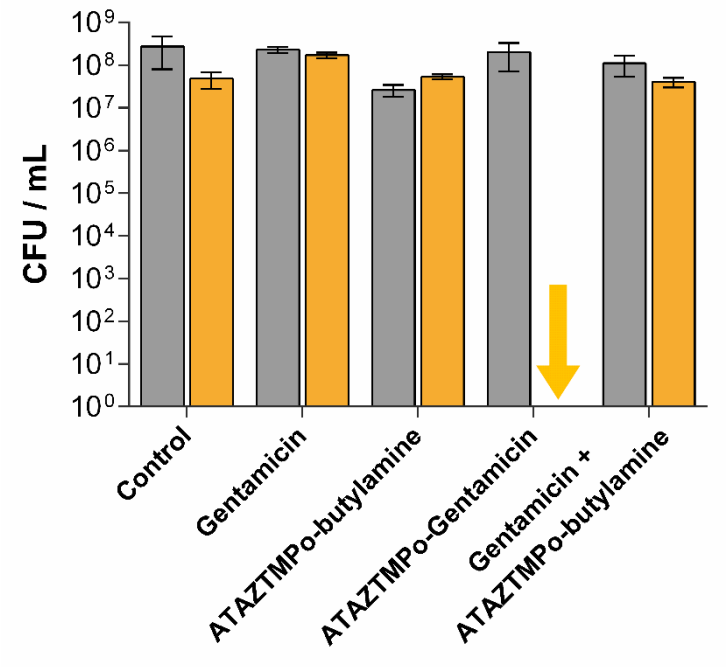

Figure 7 *E. coli* photoinactivation studies in PBS upon red light irradiation (λ = 638 ± 9 nm) (orange bars). Grey bars represent dark controls. ATAZTMPo-butylamine was added from a 5 mM stock in *N,N*-dimethylacetamide. Light doses: 45 $J \cdot cm^{-2}$. Working concentration: 8 μM. Incubation time: 1 h. Data correspond to the mean ± SD after performing three triplicates.

In order to further explore the antimicrobial effect of ATAZTMPo-gentamicin, photoinactivations were performed upon different concentrations and light fluences against *E. coli* (Figure 8, left

panel) and *S. aureus* (Figure 8, right panel). Among the whole conditions tested, the best ratio concentration/light dose with the highest antibacterial activity was found for *S. aureus* at 80 nM (45 J·cm^{-2}) or 800 nM (30 J·cm^{-2}), where the strains were completely eliminated. Curiously, in contrast with the tendency observed for bacterial inactivation with gentamicin alone (see Figure S7), photoinactivations of *E. coli* required more amount of conjugate and higher light-fluences to observe significant photosensitizing activity against the bacterial cells. Thus, complete killing was observed at 800 nM upon irradiation with 45 J·cm^{-2} of red light, whereas, a smaller killing efficiency (5 $\log_{10}$) was detected when exposed to 30 J·cm^{-2}. Noteworthy, the dark toxicity in both strains was below 1-$\log_{10}$ CFU mL^{-1}, a desired characteristic for aPDT photoantimicrobials.

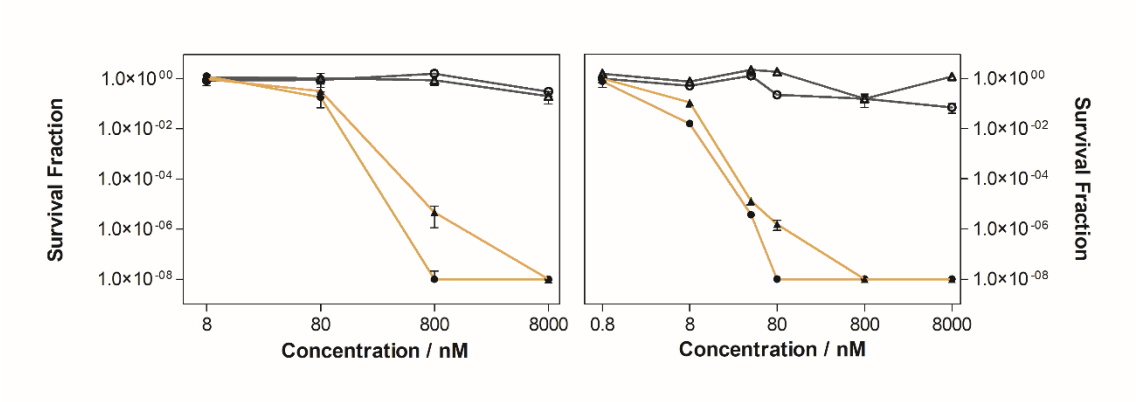

Figure 8 *E. coli* (left panel) and *S. aureus* (right panel) photoinactivation studies with ATAZTMPo-gentamicin upon red light irradiation (λ = 638 ± 9 nm). Light doses: 30 J·cm^{-2} (filled triangles), 45 J·cm^{-2} (filled circles). Working concentrations: 0.8 (only for *S. aureus*), 8, 80, 800 and 8000 nM. Incubation time: 2 h. Dark controls are represented with grey empty symbols. Data correspond to the mean ± SD after performing three triplicates.

Experiments on mammalian (HeLa) cells show that this conjugate does not present any dark toxicity at the highest concentration tested (8 μM) even after 24 h incubation, conditions much harsher than those used in the bacteria photoinactivation studies (1h incubation; data not shown).

3. Discussion and Conclusions

A novel straightforward synthesis of TMPo, that reduces from nine to six the number of steps necessary to obtain this compound, has been described. Key to this development has been the one-pot synthesis of the unprecedented *β,β'*-alkoxyalkyl-2,2'-bipyrrole from an alkoxyalkyl Michael acceptor

via a 2-(trimethylstannyl)-pyrrole intermediate. Furthermore, a click reaction between 9-ITMPo derivative and the antibiotic gentamicin has afforded a cyclised photoactive ATAZTMPo-gentamicin conjugate as a novel antimicrobial agent for aPDT. The *in vitro* photoinactivations indicate that ATAZTMPo-gentamicin is a powerful broad-spectrum near-IR photoantimicrobial agent devoid of dark toxicity and effective at submicromolar concentrations. Stemming from the results observed, the antibiotic moiety of the conjugate does not seem to exert any bactericidal effect; all cell death being attributable to the photodynamic activity of the porphycene. Rather, gentamicin enhances the solubility of the porphycene and endows it with amphiphilic character. We suspect that this allows the conjugate to cross the bacterial wall, causing damage not only to the outer wall, as the butyl conjugate would also do, but also to the inside of the bacteria, and therefore exhibiting a larger biological activity.

These promising results are evidenced when compared to previous antibacterial studies reported in the literature which used TMPo, or by combining gentamicin with other PSs. For instance, Masiera and co-workers required 5 μM of TMPo in Pluronic F-127 solution and 54 $J \cdot cm^{-2}$ light-dose to effectively inactive *E. faecalis*,[11] or Polo et al. observed about 4 $\log_{10}$ of bacterial lethality using 1 μM of TMPo linked to oligomeric polylysine residues in Gram-positive (*S. aureus*) and Gram-negative (*E. coli*) bacteria.[13] Gentamicin (3 μM) has been previously been combined with 5-aminolevulinic acid (5-ALA) aPDT, against *S. aureus* biofilms, resulted in 50% of lethality when irradiated with 250 $J \cdot cm^{-2}$.[48] Recently, Pérez-Laguna and co-workers[49] described a synergistic bactericidal effect against *S. aureus* by combination of 1.5-15 μM gentamicin with 30-70 nM Rose-Bengal under irradiation with a 37 $J \cdot cm^{-2}$ light-dose, reducing the bacteria growth by 6 $\log_{10}$.

Data for PS-antibiotic conjugates are scarce. Some few examples, such as porphyrin derivatives linked to antimicrobial peptides[21,50,51] or Rose-Bengal bound to Kanamycin[52] have been reported, where the concentrations of the corresponding conjugate needed to induce significant photosensitizing activity (1.5 - 80 μM) were much higher than that of ATAZTMPo-gentamicin conjugate (in the nanomolar range).

In summary, the photoinactivations performed with the novel ATAZTMPo-gentamicin conjugate described here, have demonstrated that the concentration of antibiotic required to achieve a bactericidal effect is significantly lower than that required for gentamicin alone, in both Gram-positive and Gram-negative bacteria. Finally, the lack of any dark toxicity observed at photochemically active doses paves the way to develop novel phototherapeutic strategies to eradicate antibiotic resistance, which has become one of the major threats to human health according to the World Health Organization (WHO).

4. Experimental Section

Chemicals

General remarks: All chemicals and dry solvents were purchased from commercial sources and used as received unless otherwise noted. Synthesis grade or HPLC–grade solvents were used for extractions and purifications. Zinc dust was activated by stirring with dilute HCl during 10-15 minutes, and then washed several times with distilled H_2O, EtOH and absolute Et_2O before rigorous drying.[53]

All reactions were monitored by TLC analysis using POLYGRAM® SIL G/UV254 pre-coated polyester sheets (0.2 mm-thickness) (Machery-Nagel). UV light was used as the visualizing agent (at λ = 254 nm or λ = 365 nm), and a 5% (w/v) ethanolic solution of phosphomolybdic acid or vanillin as developing agents. Flash column chromatography was carried out with the indicated solvents using flash-grade silica-gel 60 Å (37-70 μm). Yields refer to chromatographically and spectroscopically pure compounds, unless otherwise stated.

NMR spectra were recorded at RT on a Varian Mercury 400 (^{1}H at 400 MHz and ^{13}C at 100.6 MHz) spectrometer. The chemical shifts (δ) are reported in parts per million (ppm) relative to the solvent signal, and coupling constants (J) are reported in Hertz (Hz). The following abbreviations are used to define the multiplicities in ^{1}H NMR spectra: s = singlet, d = doublet, t = triplet, q = quartet, dd = doublet of doublets, ddd = doublet of doublet of doublets, m = multiplet, br = broad signal and app = apparent, or combinations of these descriptive names. Carbon spectra assignments are supported by

HSQC editing. Infrared spectra were recorded in a Nicolet Magna 560 FTIR spectrophotometer. Values are reported in wave numbers (cm^{-1}). Mass Spectrometry (MS) for reported compounds was conducted on an Agilent Technologies 5975 mass spectrometer operating in electron ionization (EI) mode at 70 eV and at 4 kV accelerating potential. New compounds were characterized by an HPLC-MS Agilent 1260 infinity Series chromatograph equipped with photodiode array detector (200–700 nm) and coupled to an Agilent 6130 quadrupole LC/MS. Separation was achieved using a XBridge™ C18 (4.6 x 75 mm, 2.5µm particle size) column. The flow rate was 1 mL/min, column temperature 45 ºC. The DAD detector was set at 380 nm matching the Soret band of porphycenes. API-ES positive ionization mode at 15 V cone voltage was used. Fragmentations were scanned from 0 to 1800 m/z. Samples (200 ppm in MeOH) were analysed using a 20 µL volume injection. *m/z* ratios are reported in atomic mass units.

Synthetic procedures

3-Methoxy-1-propanal (2) To a solution of 3-methoxy-1-propanol **1** (25 mL, 262.0 mmol) in 700 mL of EtOAc, 2-iodoxybenzoic acid (IBX) (88 g, 315.0 mmol, prepared according to literature)[30] was added in one portion; the mixture was refluxed overnight and then cooled to RT. The white precipitate was removed by filtration through a Celite® pad and further rinsed with 3 x 100 mL of EtOAc. The solvent of the organic layers was distilled at 80 ºC (atm) giving 3-methoxy-1-propanal as unique product (19.6 g, 222.0 mmol, 85%). The physical and spectroscopic data of 3-methoxy-1-propanal **2** were identical to those reported in the literature.[31,54]

TLC (CH_2Cl_2:MeOH; 95:5), Rf: 0.46. ^{1}H NMR ($CDCl_3$): δ 9.79 (td, J = 2.0, 1.0, 1H), 3.72 (t_{app}, J = 6.0, 2H), 3.36 (s, 3H), 2.66 (td, J = 6.0, 2.0, 2H). ^{13}C NMR ($CDCl_3$): δ 201.2 (C), 66.4 (CH_2), 59.1 (CH_3), 44.0 (CH_2).

(*E*)-Ethyl 5-methoxypent-2-enoate (3) Triethyl phosphonoacetate (64 mL, 306.0 mmol) was slowly added to a suspension of NaH (60% in mineral oil, 13 g, 327.0 mmol) in anhydrous THF (400 mL) at 0 °C. After 30 min of stirring at 0 ºC, a solution of 3- methoxy-1-propanal **2** (19 g, 215.0 mmol) in anhydrous THF (80 mL) was added. The reaction mixture was stirred at 0 °C for 1.5 h before being quenched by saturated NH_4Cl (200 mL). The product was extracted with EtOAc (3 x 150 mL). The

combined extracts were washed with brine, dried and concentrated. The crude was redissolved in cyclohexane and the mixture was washed with saturated NH_4Cl solution (3 x 100 mL), brine (3 x 100 mL) and water (3 x 100 mL). The organic extracts were dried over anhydrous $MgSO_4$ and concentrated under reduced pressure to afford ethyl 5-methoxypent-2-enoate as a yellowish oil (26 g (*E:Z*; 98:2), 162 mmol, 75%) without further purification. The physical and spectroscopic data of ethyl 5-methoxypent-2-enoate **3** were identical to those reported in the literature.[55]

TLC (Cyclohexane:EtOAc; 8:2), Rf: 0.44 (*E*); 0.52 (*Z*). ^{1}H NMR ($CDCl_3$): (Data for only *E*) δ 6.95 (dt, J = 15.5, 7.0, 1H), 5.89 (dt, J = 15.5, 1.5 Hz, 1H), 4.18 (q, J = 7.0, 2H), 3.50 (t, J = 6.5, 2H), 3.35 (s, 3H), 2.52 – 2.42 (qd, J = 6.5, 1.5, 2H), 1.28 (t, J = 7.0 Hz, 3H). ^{13}C NMR ($CDCl_3$): (Data for only *E*) δ 166.6 (C), 145.7 (CH), 123.1 (CH), 70.9 (CH_2), 60.4 (CH_2), 58.9 (CH_2), 32.7 (CH_2), 14.4 (CH_3).

Diethyl 4,4'-bis(2-methoxyethyl)-1*H*,1'*H*-[2,2'-bipyrrole]-3,3'-dicarboxylate (4) *n*-BuLi (1.6 M in hexane, 96 mL, 154.0 mmol) was added to a solution of *p*-toluenesulfonylmethyl isocyanide (TosMIC) (16.7 g, 85.0 mmol) in anhydrous THF (250 mL) at -78 °C. After 5 min of stirring at -78 °C, 125 mL of Me_3SnCl (1 M in THF, 125.0 mmol) was added dropwise. After another 5 min of stirring at -78 °C, a solution of ethyl 5-methoxypent-2-enoate **3** (9.0 g, 57.0 mmol) in anhydrous THF (100 mL) was added dropwise. The temperature of the reaction mixture was allowed to rise to RT in 30 min, and stirring was continued for 2 h. To this solution, 14.0 g of $Cu(NO_3)_2{\cdot}3H_2O$ (57.0 mmol) was added in a single portion. The mixture was stirred at RT for 40 minutes, and then added an additional 57.0 mmol of $Cu(NO_3)_2{\cdot}3H_2O$. The solvent was removed under reduced pressure and the residue was dissolved in EtOAc. The organic layer was washed with 10% ammonia (3 x 500 mL), water (3 x 500 mL) and brine. The solvent was dried over $MgSO_4$ and concentrated under reduced pressure. The crude was purified by flash chromatography (CH_2Cl_2:EtOAc; stepwise gradient from 0 to 5% of EtOAc) to yield the corresponding bipyrrole **4** as a yellow solid (2.7 g, 7.0 mmol, 25%).

TLC (Cyclohexane:EtOAc; 8:2), Rf: 0.67. ^{1}H NMR ($CDCl_3$): δ 13.61 (br s, 2H), 6.66 (d, J = 2.5, 2H), 4.36 (q, J = 7.0, 4H), 3.59 (t, J = 7.0, 4H), 3.37 (s, 6H), 3.03 (td, J = 7.0, 1.0, 4H), 1.41 (t, J = 7.0, 6H). ^{13}C NMR ($CDCl_3$): δ 168.8 (C), 130.6 (C), 124.0 (C), 117.4 (CH), 109.6 (C), 73.5 (CH_2), 60.9 (CH_2), 58.8 (CH_3), 28.6 (CH_2), 14.4 (CH_3). IR (KBr): υ, cm^{-1} 3500–3200 (st N–H), 2978 (=C-H),

2930, 2891, 2869 (st C-H), 1652 (st C=O), 1564 (st C=C), 1417, 1181 (st as CO-O), 1119 (st as O-C-C). ESI-MS *m/z* $C_{20}H_{28}N_2O_6$ $[M+Na]^+$ Found: 415.1795; Calculated: 415.18; $[M+H]^+$ Found: 393.1880; Calculated: 393.20.

4,4'-Bis(2-methoxyethyl)-1*H*,1'*H*-2,2'-bipyrrole (5) Diethyl 4,4'-bis(2-methoxyethyl)-1*H*,1'*H*-[2,2'-bipyrrole]-3,3'-dicarboxylate **4** (2.7 g, 6.8 mmol), ethylene glycol (50 mL) and sodium hydroxide (5.4 g, 136 mmol) were combined in a 500 mL two-necked round-bottom flask fitted with a reflux condenser. The system was degassed for 1 hour with a stream of N_2, and the mixture was heated to 180 ºC for 90 minutes under N_2 atmosphere. The mixture was allowed to cool to 100 ºC and then 100 mL of water (previously degassed) was added. The resulting slurry was allowed to cool to RT and the mixture was extracted with CH_2Cl_2 (3 x 300 mL), water (3 x 300 mL) and brine. The organic extracts were dried over anhydrous $MgSO_4$ and concentrated under reduced pressure to afford the corresponding bipyrrole as a dark-green powder without further purification (1.4 g, 5.8 mmol, 85%). The physical and spectroscopic data of 4,4'-bis(2-methoxyethyl)-1*H*,1'*H*-2,2'-bipyrrole *5* were identical to those reported in the literature.[56]

TLC (Cyclohexane:EtOAc; 8:2), Rf: 0.31. ^{1}H NMR ($CDCl_3$): δ 8.00 (br s, 2H), 6.59 – 6.55 (m, 2H), 6.07 (dd, J = 2.5, 1.5, 2H), 3.58 (t, J = 7.0, 4H), 3.38 (s, 6H), 2.75 (t, J = 7.0, 4H). ^{13}C NMR ($CDCl_3$): δ 126.1 (C), 121.8 (C), 115.4 (CH), 104.3 (CH), 73.9 (CH_2), 58.7 (CH_3), 27.6 (CH_2).

IR (KBr): v, cm^{-1} 3600-3200 (st N–H), 2924, 2860 (st C-H), 1109 (st C-O). MS (EI) *m/z* (rel intensity) $C_{14}H_{20}N_2O_2$ 248.2 (100%).

4,4'-Bis(2-methoxyethyl)-1*H*,1'*H*-[2,2'-bipyrrole]-5,5'-dicarbaldehyde (6) To a solution of 1.2 g (5.0 mmol) of 4,4'-bis(2-methoxyethyl)-1*H*,1'*H*-2,2'-bipyrrole **5** in dry DMF (25 mL), phosphoryl chloride (1.7 mL, 19.0 mmol) was added dropwise at 0 ºC, under argon. The solution was heated to 60 ºC for 1 h and then cooled at RT. The resulting mixture was chilled in an ice/water bath while adding a solution of 28 g of NaOAc in 220 mL of water. This biphasic mixture was then heated at 85 ºC for 1 hour, wherein the dialdehyde precipitated out as yellow flakes. The suspension was cooled to 0 ºC, filtered and the residue was washed with cold water. The precipitate was then purified by flash column chromatography (EtOAc; 100%) to yield the desired dialdehyde as a yellow powder (1.2 g,

4.0 mmol, 80%). The physical and spectroscopic data of 4,4'-bis(2-methoxyethyl)-1*H*,1'*H*-[2,2'-bipyrrole]-5,5'-dicarbaldehyde **6** were identical to those reported in the literature.[56]

TLC (EtOAc), Rf: 0.5. ^{1}H NMR ($CDCl_3$): δ 12.26 (br s, 2H), 9.70 (s, 2H), 6.58 (d, J = 2.5, 2H), 3.65 (t, J = 6.5, 4H), 3.39 (s, 6H), 3.07 (t, J = 6.5, 4H). ^{13}C NMR ($CDCl_3$): δ 177.8 (CH), 136.2 (C), 131.7 (C), 130.7 (C), 111.9 (CH), 73.0 (CH_2), 58.9 (CH_3), 26.2 (CH_2). IR (KBr): v, cm^{-1} 3268 (st N–H), 3175 (st =C-H), 2982, 2926, 2876 (st C-H), 1649, 1607 (st C=O), 1116 (st C-O).

MS (EI) *m/z* (rel intensity) $C_{16}H_{20}N_2O_4$ 304.2 (100%).

2,7,12,17-Tetrakis(methoxyethyl)porphycene (TMPo) To a slurry of low-valent titanium reagent, generated by reduction of titanium tetrachloride (3.6 mL, 33.0 mmol) in anhydrous THF (200 mL) with activated zinc (4.3 g, 65.5 mmol) and CuCl (1.0 g, 10.0 mmol) by refluxing 3 h, a solution of 4,4'-bis(2-methoxyethyl)-1*H*,1'*H*-[2,2'-bipyrrole]-5,5'-dicarbaldehyde **6** (400 mg, 1.3 mmol) in anhydrous THF (200 mL) was added dropwise slowly over 1 h under reflux conditions with vigorous stirring. The reaction mixture was heated under reflux for an additional 1 h and then hydrolyzed by slow addition of 10% aqueous potassium carbonate (ca. 175 mL) to the ice cooled reaction mixture. The reaction mixture was stirred with 150 mL of CH_2Cl_2 under oxygen atmosphere for 30 min and then filtered through Celite® pad to remove the metal excess. The residue was extracted with 200 mL of CH_2Cl_2, and the combined organic layer were washed with water (3 x 200 mL). Following drying over anhydrous $MgSO_4$, the solvent was rotoevaporated and the residue was chromatographed on silica gel ($CHCl_3$; 100%) to afford a dark violet-blue fraction. The red fluorescing compound was finally purified by trituration with hot hexane giving the TMPo porphycene as long violet needles. Yield: 25% (90 mg, 150 µmol). The physical and spectroscopic data of TMPo were identical to those reported in the literature.[56]

TLC ($CHCl_3$), Rf: 0.1. ^{1}H NMR ($CDCl_3$): δ 9.72 (s, 4H), 9.34 (s, 4H), 4.34 – 4.31 (m, 16H), 3.62 (s, 12H), 3.10 (br s, 2H). ^{13}C NMR ($CDCl_3$): δ 143.7 (C), 141.0 (C), 134.3 (C), 123.8 (CH), 110.9 (CH), 74.2 (CH_2), 59.2 (CH_3), 29.0 (CH_2). IR (KBr): v, cm^{-1} 3600-3300 (st N-H), 2868, 2806 (st C–H), 1561 (st C=C), 1460, 1391 (as C-H), 1117 (st C-O). MS (EI) *m/z* (rel intensity) $C_{32}H_{38}N_4O_4$ 542.3 (54%).

9-Nitro-2,7,12,17-tetrakis(methoxyethyl)porphycene (9-NTMPo) $AgNO_3$ (50 mg, 275 μmol) was added in one portion to a solution of 2,7,12,17-tetrakis(methoxyethyl)porphycene (150 mg, 275 μmol) in AcOH/CH_2Cl_2 100/70 mL. The mixture was vigorously stirred at 55 ºC for 20 min, monitoring the reaction conversion by TLC (CH_2Cl_2:EtOAc; 75:25). The resulting dark green mixture was cooled down at RT and filtered through a Celite® pad. The combined filtrate was washed with H_2O, the organic layer was neutralised with an aqueous solution of $NaHCO_3$ (10%), dried over anhydrous $MgSO_4$ and concentrated under reduced pressure. Flash column chromatography purification with silica-gel (CH_2Cl_2:EtOAc; stepwise gradient from 0 to 30% of EtOAc) gave compound 9-NTMPo as a dark green solid (160 mg, 275 μmol, 100%). The physical and spectroscopic data of 9-NTMPo were identical to those reported in the literature.[35]

TLC (CH_2Cl_2:EtOAc; 75:25), Rf: 0.2. ^{1}H NMR ($CDCl_3$): δ 9.52 (s, 1H), 8.93 (s, 1H), 8.81 (dd, J_{AB} = 12.0, 2H), 8.66 (s, 1H), 8.48 (s, 1H), 8.35 (s, 1H), 4.26 (t, J = 6.5, 2H), 4.16 (t, J = 7.0, 4H), 4.11 (t, J = 7.0, 2H), 4.02 (t, J = 6.5, 2H), 3.99 – 3.89 (m, 6H), 3.68 (s, 3H), 3.61 (s, 3H), 3.61 (s, 3H), 3.59 (s, 3H), 1.45 (s, 1H), 0.89 (s, 1H). ^{13}C NMR ($CDCl_3$): δ 143.9 (C), 143.4 (C), 141.8 (C), 141.7 (C), 140.8 (C), 138.0 (C), 137.5 (C), 137.3 (C), 135.8 (C), 135.4 (C), 134.7 (C), 132.9 (C), 132.0 (C), 126.5 (CH), 123.8 (CH), 122.9 (CH), 122.8 (CH), 112.0 (CH), 110.6 (CH), 105.3 (CH), 73.5 (3 x CH_2), 73.1 (CH_2), 59.1 (3 x CH_3), 59.0 (CH_3), 29.2 (CH_2), 28.5 (CH_2), 28.4 (CH_2). IR (KBr): v, cm^{-1} 2821, 2869 (st C–H), 1560 (st C=C), 1519 (as NO_2), 1461 (δ C-H), 1336 (sym NO_2), 1190 (st C-N), 1117 (st C-O), 998, 960, 870, 812. MS (EI) *m/z* (rel intensity) $C_{32}H_{37}N_5O_6$ 587.3 (60%)

9-Amino-2,7,12,17-tetrakis(methoxyethyl)porphycene (9-ATMPo) An aqueous solution of NaOH 5 M (55 mL) was added to a solution of 9-NTMPo (160 mg, 275 μmol) in CH_2Cl_2 (100 mL), followed by the addition of 65 mL of $Na_2S_2O_4$ (11.4 g, 65 mmol) dissolved in water. The two-phase mixture was heated under reflux for 45 min, monitoring the reaction conversion by TLC (CH_2Cl_2:EtOAc; 75:25). The resulting crude was washed with water and the organic phase was dried over anhydrous $MgSO_4$ and concentrated under reduced pressure. The resulting dark blue solid (145 mg, 260 μmol, 95%) was used without further purification. The physical and spectroscopic data of 9-NTMPo were identical to those reported in the literature.[35]

TLC (CH_2Cl_2:EtOAc; 75:25), Rf: 0.3. ^{1}H NMR ($CDCl_3$): δ 9.41 (d, J = 11.0, 1H), 9.09 (d, J = 11.0, 1H), 8.96 (s, 1H), 8.94 (s, 1H), 8.84 (s, 1H), 8.81 (s, 1H), 8.42 (s, 1H), 6.22 (br s, 2H), 5.46 (s, 1H), 4.90 (s, 1H), 4.30 – 4.16 (m, 8H), 4.13 (dd, J = 8.0, 6.5, 4H), 3.90 (dt, J = 11.5, 6.5, 4H), 3.61 (s, 3H), 3.60 (s, 3H), 3.55 (s, 3H), 3.46 (s, 3H).b ^{13}C NMR ($CDCl_3$): δ 145.8 (C), 145.3 (C), 141.6 (C), 141.5 (C), 140.8 (C), 139.0 (C), 138.3 (C), 136.8 (C), 136.6 (C), 133.6 (C), 132.6 (C), 132.5 (C), 132.4 (C), 124.5 (CH), 123.6 (CH), 122.5 (CH), 121.1 (CH), 114.0 (CH), 106.9 (CH), 101.2 (CH), 75.6 (CH_2 x 3), 74.5 (CH_2), 74.0 (CH_2 x 3), 73.6 (CH_2 x 2), 59.4 (CH_3), 59.1 (CH_3 x 3), 31.1 (CH_2), 28.8 (CH_2 x 2), 28.75 (CH_2 x 2), 28.7 (CH_2 x 2). IR (KBr): v, cm^{-1} 3350, 3241 (st N-H), 2921, 2865 (st C-H), 1646 (δ N-H), 1553 (st arom C=C), 1463, 1357 (δ C-H), 1326, 1188 (st C-N), 1113 (st C-O), 993, 891, 812, 625, 470. MS (EI) *m/z* (rel intensity) $C_{32}H_{39}N_5O_4$ 557.3 (70%).

9-Isothiocyanate-2,7,12,17-tetrakis(methoxyethyl)porphycene (9-ITMPo) 1,1′-Thiocarbonyldi-2(1H)-pyridone (125 mg, 540 µmol) was added to a solution of 9-ATPPo (100 mg, 180 µmol) in CH_2Cl_2 (25 mL). The mixture was stirred during 16 h at room temperature. The solvent was evaporated and the residue was chromatographed on silica gel (EtOAc; 100%) to afford a dark blue-green compound (85 mg, 140 µmol, 80%).

TLC (EtOAc), Rf: 0.42. ^{1}H NMR ($CDCl_3$): δ 9.66 (d, J_{AB} = 11.0, 1H), 9.62 (d, J_{AB} = 11.0 Hz, 1H), 9.35 (s, 1H), 9.22 – 9.19 (m, 2H), 9.16 (s, 1H), 9.14 (s, 1H), 4.37 – 4.21 (m, 14H), 4.15 (t_{app}, J = 6.5, 2H), 3.63 (s, 3H), 3.62 (s, 3H), 3.62 (s, 6H), 3.52 (br s, 1H), 2.79 (br s, 1H). ^{13}C NMR ($CDCl_3$): δ 143.9 (C), 143.3 (C), 141.0 (C), 140.5 (C), 140.2 (C), 139.3 (C), 138.3 (C), 137.6 (C), 135.1 (C), 133.7 (C), 133.5 (C), 133.1 (C), 132.7 (C), 124.7 (CH), 123.6 (CH), 123.4 (CH), 122.8 (CH), 114.9 (C), 111.4 (CH), 111.1 (CH), 110.4 (CH), 73.9 (CH_2), 73.3 (CH_2), 72.9 (CH_2), 59.2 (2 x CH_3), 59.1 (2 x CH_3), 30.6 (CH_2), 28.8 (2 x CH_2), 28.2 (CH_2). IR (KBr): v, cm^{-1} 3439 (st N-H), 2921, 2870 (st C–H), 2134 (st SC≡N), 1116 (st C-O), 966 (st sym N=C=S), 889, 811 (st C-S). ESI-MS *m/z* $C_{33}H_{37}N_5O_4S$ $[M+H]^+$ Found:600.3877; Calculated: 600.26.

2-gentamicin-thiazolo[4,5-*c*]2,7,12,17-tetrakis(methoxyethyl)porphycene (ATAZTMPo-gentamicin) To a mixture of gentamicin sulphate (500 mg, 830 µmol) and K_2CO_3 (150 mg, 1.1 mmol) in ethanol (10 mL), 9-ITMPo (5.0 mg, 8 µmol) in ethanol (2 mL) was added dropwise. The

resulting solution was stirred at RT for 5 days until no conversion was observed by TLC. The green mixture was concentrated under reduced pressure, and the resulting crude was purified by flash column chromatography on C18-RP silica-gel (glacial acetic acid:Methanol; 5:95); stepwise gradient from 0 to 100% of MeOH) to afford the desired ATAZTMPo-gentamicin conjugate in 75% (8 mg, 6 μmol) yield. The pure fraction isolated was analysed by RP-HPLC-MS in gradient elution mode applying the following gradient profile: 0 - 0.5 min: 100% A; 0.5 - 2 min: 0 - 100% B; 2 - 7 min: 100% B; 7 - 9 min: 0 - 100% A; 9 - 15 min: 100% A; Mobile phase A: Water; B: MeOH; both with 0.1% formic acid (v/v). ATAZTMPo-gentamicin, as a mixture of congeners due to gentamicin, was isolated at retention time around 3.4 min (Figure S1). The MS survey scan at retention time of 3.576 min confirmed the single-conjugate for the most abundant charge state of z = 1 and z = 2 of ATAZTMPo-(C_1)gentamicin congener, as well as the pick at 3.375 min the z = 1 and z = 2 of ATAZTMPo-($C_{1,1a}$)gentamicin congener can be observed along with other conjugate fragmentations (Figure S2).

TLC ($CHCl_3$:MeOH:$NH_{3\ (liq\ 30\%)}$; 70:30:10), Rf: 0.82. ESI-MS *m/z* ATAZTMPo-(C_1)gentamicin $C_{53}H_{76}N_{10}O_{11}S$ $[M+H]^+$ Found: 1061.5555; Calculated: 1061.5494; $[M+2H]^{2+}$ Found: 531.2758; Calculated: 531.2780. ATAZTMPo-($C_{1,1a}$)gentamicin $C_{52}H_{74}N_{10}O_{11}S$ $[M+H]^+$ Found: 1047.5403; Calculated: 1047.5338; $[M+2H]^{2+}$ Found: 524.2782; Calculated: 524.2703.

2-*N*-butylaminothiazolo[4,5-*c*]2,7,12,17-tetrakis(methoxyethyl)porphycene (ATAZTMPo-butylamine) *N*-butylamine (0.62 mL, 6.2 mmol) was added dropwise to a solution of 9-isothiocyanate-2,7,12,17-tetrakis(methoxyethyl)porphycene (9-ITMPo, 15 mg, 0.025 mmol) in CH_2Cl_2 (5 mL). The mixture was stirred 24 h at room temperature. Then, the mixture was concentrated under reduced pressure and the crude was purified by flash column chromatography (CH_2Cl_2:MeOH; stepwise gradient from 0 to 2% of MeOH) to afford the green ATAZTMPo-butylamine in 80% (13 mg, 0.02 mmol) yield.

TLC (CH_2Cl_2:MeOH; 95:5), Rf: 0.7. ^{1}H NMR ($CDCl_3$): δ 9.43 (d, J = 11.0, 1H), 9.31 (d, J = 11.0, 1H), 9.15 – 9.03 (m, 2H), 8.98 (s, 1H), 8.79 (s, 1H), 5.65 (t, J = 5.5, 1H), 4.77 (s, 1H), 4.37 (t_{app}, J = 7.0 Hz, 2H), 4.32 – 4.16 (m, 8H), 4.05 (t, J_{app} = 7.0 Hz, 2H), 3.88 (s, 1H), 3.72 - 3.64 (m, 2H), 3.61 (s,

3H), 3.60 (s, 3H), 3.59 – 3.57 (m, 2H), 3.57 (s, 3H), 3.54 (s, 3H), 1.86 (dt, J = 15.0, 7.5, 2H), 1.61 (td, J = 15.0, 7.5, 2H), 1.10 (t, J = 7.5, 3H). ^{13}C NMR ($CDCl_3$): δ 164.0 (C), 143.6 (C), 142.9 (C), 142.1 (C), 140.3 (C), 139.4 (C), 139.2 (C), 138.8 (C), 137.2 (C), 136.1 (C), 135.4 (C), 133.2 (C), 132.7 (C), 130.1 (C), 125.3 (CH), 124.0 (CH), 123.2 (CH), 123.0 (CH), 120.5 (C), 111.3 (CH), 108.7 (CH), 74.1 (CH_2), 73.9 (CH_2), 72.3 (CH_2), 59.0 (CH_3), 58.9 (CH_3), 58.8 (CH_3), 45.2 (CH_2), 32.4 (CH_2), 31.8 (CH_2), 31.4 (CH_2), 28.7 (CH_2), 28.6 (CH_2), 20.3 (CH_2), 13.9 (CH_3). IR (KBr): υ, cm^{-1} 3390 (st N-H), 2921, 2870 (st C-H), 1640 (δ N-H), 1550 (st arom C=C), 1465, 1360 (δ C-H), 1326, 1190 (st C-N), 1115 (st C-O), 985, 890, 812. ESI-MS *m/z* $C_{37}H_{46}N_6O_4S$ $[M+Na]^+$ Found: 693.3204; Calculated: 693.3199; $[M+H]^+$ Found: 671.3377; Calculated: 671.3379.

Spectroscopic techniques

All spectroscopic measurements were carried out in 1 cm quartz cuvettes (Hellma, Germany) in air-saturated solutions, unless otherwise stated, at room temperature using spectroscopic grade solvents. Absorption spectra were recorded using a double beam UV-Vis-NIR Varian Cary 6000i spectrophotometer (Varian, Palo Alto, CA, USA). Absorption coefficients were derived from the slopes of Beer-Lambert plots.

Fluorescence emission and excitation spectra were registered using a a Spex Fluoromax-4 spectrofluorometer (Horiba Jobin-Yvon, Edison, NJ, USA). Fluorescent quantum yields were determined by plotting the integrated fluorescent intensity of a series of solutions of increasing concentration versus the amount of light absorbed ($1\text{-}10^{-Abs}$), obtaining a linear correlation. By means of Equation 1, slopes of the desired compound and reference (*meso*-tetraphenylporphyrin; Φ_F = 0.11)[41] were compared, and corrected by the refractive index of the solvents used.

$$\Phi_F = \frac{Slope_{Sample} \cdot n^2_{Sample}}{Slope_{Reference} \cdot n^2_{Reference}} \qquad (1)$$

Time-resolved fluorescence decays were measured using a Fluotime 200 time-correlated fluorescence lifetime spectrophotometer (PicoQuant GmbH, Berlin, Germany), equipped with a red sensitive photomultiplier. Excitation was achieved by means of a 596 nm picosecond diode laser working at 10

MHz repetition rate. The counting frequency was always below 1%. Fluorescence lifetimes were analysed using PicoQuant FluoFit 4.6.6 data analysis software.

Transient absorption spectra (Figure S4) were monitored by nanosecond laser flash photolysis using a Q-switched Nd:YAG Laser (Surelite I-10, Continuum) with right-angle geometry and an analysing beam produced by a Xe lamp (PTI, 75 W) in combination with a dual-grating monochromator (mod. 101, PTI) coupled to a UV-Vis radiation detector (PTI 710). The signal was fed to a Lecroy WaveSurfer 454 oscilloscope for digitizing and averaging (typically 10 shots) and finally transferred to a PC for data storage and analysis.

Singlet oxygen generation was studied by time-resolved near-infrared phosphorescence by means of a customised setup.[57] Briefly, a pulsed Nd:YAG laser (FTSS355-Q, Crystal Laser, Berlin, Germany) working at 1 kHz repetition rate at 355 nm (0.5 μJ per pulse) was used to excite the sample. A 1064-nm rugate notch filter (Edmund Optics) and an uncoated SKG-5 filter (CVI Laser Corporation) were placed in the laser path to remove any NIR emission. The light emitted by the sample was filtered with a 1000-nm long-pass filter (Edmund Optics) and later by a narrow bandpass filter at 1275 nm (BK-1270-70-B, bk Interferenzoptik). A thermoelectric-cooled NIR-sensitive photomultiplier tube assembly (H9170-45, Hamamatsu Photonics, Hamamatsu, Japan) was used as detector. Photon counting was achieved with a multichannel scaler (NanoHarp 250, PicoQuant). The time dependence of the $^1O_2$ phosphorescence with the signal intensity $S(t)$ is described by Equation 2, in which τ_T and τ_Δ are the lifetimes of the photosensitizer triplet state and of $^1O_2$ respectively, and S_0 a preexponential parameter proportional to Φ_Δ.

$$S_{1275}(t) = S_{1275}(0) \times \frac{\tau_\Delta}{\tau_\Delta - \tau_T} \times \left(exp^{-t/\tau_\Delta} - exp^{-t/\tau_T} \right) \qquad (2)$$

The plotting of S_0 versus the absorbed energy at different concentrations yields also a linear relationship. The Φ_Δ values of the different samples were obtained by comparison of the slopes of such plots with an appropriate reference compound using Equation 3.

$$\Phi_{\Delta,\text{sample}} = \Phi_{\Delta,\text{ref}} \times \frac{Slope_{sample}}{Slope_{ref}} \qquad (3)$$

Microbial strains, culture conditions and photodynamic inactivation studies

The microorganisms studied were *Staphylococcus aureus* ATCC 29213 as a Gram-positive model and *Escherichia coli* ATCC 25922 as Gram-negative bacteria.

Bacterial cells were grown overnight in an orbital shaker at 37 °C in Tryptic Soy Broth (TSB) medium. An aliquot was then suspended in fresh TSB and set to grow in exponential phase at 37 °C to achieve approximately 10^8 colony forming units ($CFU \cdot mL^{-1}$). They were later centrifuged (5000 rpm, 10 min) and resuspended in PBS (pH = 7.4). The cells were incubated with the drug, delivered in PBS, in the dark for 1 hour under the same growth conditions.

Three independent experiments were done for each photoinactivation treatment, which in turn was carried out in duplicate. The average and SD values were calculated.

Cells were then irradiated from the top in 96-well plates by means of a LED-lamp (Sorisa Photocare; 635 ± 15 nm; 17 $mW \cdot cm^{-2}$). The irradiance of the lamp was regularly monitored with an Ophir AN/2 Laser Power Meter (Ophir Optronics Solutions Ltd, Har Hotzvim, Israel) to ensure the light dose delivered.

Since no significant statistical difference was obtained when the photoinactivation was performed with and without removal of the excess of ATAZTMPo-gentamicin or the PS by centrifugation (data not shown), the procedure was followed without removal of the excess of the conjugate.

Controlling the cell irradiation without PS was also performed in order to exclude any inactivation due to light or heating effects, along with the evaluation of the toxicity of ATAZTMPo-gentamicin in the dark and controls using gentamicin. After illumination, the samples were serially diluted and streaked on agar plates and incubated in the dark for 18 h at 37 °C.

5. Associated Content

Supporting Information

Bacterial inactivations with gentamicin, characterisations, and further spectroscopic data (PDF).

6. Acknowledgements

This work was supported by the Spanish Ministerio de Economia y Competitividad through grant No. CTQ2016-78454-C2-1-R.

C. H. thanks the SUR del DEC de la Generalitat de Catalunya and the FSE for his predoctoral fellowship (grants No. 2017 FI_B_00617, 2018 FI_B1 00174 and 2019 FI_B2 00167).

7. References

(1) Wellcome Trust and UK Department of Health. Review on antimicrobial resistance. Tackling drug-resistant infections globally. 2014. http://amr-review.org/ (accessed May 16, 2018).

(2) Cassini, A.; Högberg, L. D.; Plachouras, D.; Quattrocchi, A.; Hoxha, A.; Simonsen, G. S.; Colomb-Cotinat, M.; Kretzschmar, M. E.; Devleesschauwer, B.; Cecchini, M.; et al. Attributable Deaths and Disability-Adjusted Life-Years Caused by Infections with Antibiotic-Resistant Bacteria in the EU and the European Economic Area in 2015: A Population-Level Modelling Analysis. *Lancet Infect. Dis.* **2019**, *19* (1), 56–66.

(3) Wainwright, M.; Maisch, T.; Nonell, S.; Plaetzer, K.; Almeida, A.; Tegos, G. P.; Hamblin, M. R. Photoantimicrobials—Are We Afraid of the Light? *Lancet Infect. Dis.* **2017**, *17* (2), e49–e55.

(4) Nonell, S.; Flors, C. *Singlet Oxygen: Applications in Biosciences and Nanosciences, Volume 1*; Nonell, S., Flors, C., Eds.; Comprehensive Series in Photochemical & Photobiological Sciences; Royal Society of Chemistry: Cambridge, 2016; Vol. 1.

(5) Nonell, S.; Flors, C. *Singlet Oxygen: Applications in Biosciences and Nanosciences, Volume 2*; Nonell, S., Flors, C., Eds.; Comprehensive Series in Photochemical & Photobiological Sciences; Royal Society of Chemistry: Cambridge, 2016; Vol. 2.

(6) Castano, A. P.; Demidova, T. N.; Hamblin, M. R. Mechanisms in Photodynamic Therapy: Part One - Photosensitizers, Photochemistry and Cellular Localization. *Photodiagnosis Photodyn. Ther.* **2004**, *1* (4), 279–293.

(7) Stockert, J.; Canete, M.; Juarranz, A.; Villanueva, A.; Horobin, R.; Borrell, J.; Teixido, J.; Nonell, S. Porphycenes: Facts and Prospects in Photodynamic Therapy of Cancer. *Curr. Med. Chem.* **2007**, *14* (9), 997–1026.

(8) Ragàs, X.; Sánchez-García, D.; Ruiz-González, R.; Dai, T.; Agut, M.; Hamblin, M. R.; Nonell, S. Cationic Porphycenes as Potential Photosensitizers for Antimicrobial Photodynamic Therapy. *J. Med. Chem.* **2010**, *53* (21), 7796–7803.

(9) Waluk, J. Spectroscopy and Tautomerization Studies of Porphycenes. *Chem. Rev.* **2017**, *117* (4), 2447–2480.

(10) Richert, C.; Wessels, J. M.; Mueller, M.; Kisters, M.; Benninghaus, T.; Goetz, A. E. Photodynamic Antitumor Agents: .Beta.-Methoxyethyl Groups Give Access to Functionalized Porphycenes and Enhance Cellular Uptake and Activity. *J. Med. Chem.* **1994**, *37* (17), 2797–2807.

(11) Masiera, N.; Bojarska, A.; Gawryszewska, I.; Sadowy, E.; Hryniewicz, W.; Waluk, J. Antimicrobial Photodynamic

Therapy by Means of Porphycene Photosensitizers. *J. Photochem. Photobiol. B Biol.* **2017**, *174*, 84–89.

(12) Lauro, F. M.; Pretto, P.; Covolo, L.; Jori, G.; Bertoloni, G. Photoinactivation of Bacterial Strains Involved in Periodontal Diseases Sensitized by Porphycene-Polylysine Conjugates. *Photochem. Photobiol. Sci.* **2002**, *1* (7), 468–470.

(13) Polo, L.; Segalla, A.; Bertoloni, G.; Jori, G.; Schaffner, K.; Reddi, E. Polylysine – Porphycene Conjugates as Efficient Photosensitizers for the Inactivation of Microbial Pathogens. *J. Photochem. Photobiol. B Biol.* **2000**, *59* (1–3), 152–158.

(14) Worthington, R. J.; Melander, C. Combination Approaches to Combat Multidrug-Resistant Bacteria. *Trends Biotechnol.* **2013**, *31* (3), 177–184.

(15) He, Y.; Huang, Y. Y.; Xi, L.; Gelfand, J. A.; Hamblin, M. R. Tetracyclines Function as Dual-Action Light-Activated Antibiotics. *PLoS One* **2018**, *13* (5), 1–15.

(16) Cahan, R.; Swissa, N.; Gellerman, G.; Nitzan, Y. Photosensitizer-Antibiotic Conjugates: A Novel Class of Antibacterial Molecules. *Photochem. Photobiol.* **2010**, *86* (2), 418–425.

(17) Pérez-Laguna, V.; Pérez-Artiaga, L.; Lampaya-Pérez, V.; García-Luque, I.; Ballesta, S.; Nonell, S.; Paz-Cristobal, M. P.; Gilaberte, Y.; Rezusta, A. Bactericidal Effect of Photodynamic Therapy, Alone or in Combination with Mupirocin or Linezolid, on Staphylococcus Aureus. *Front. Microbiol.* **2017**, *8*, 1002–1011.

(18) Nisnevitch, M.; Valkov, A.; Nakonechny, F.; Gutterman, M.; Nitzan, Y. Antibiotics Combined with Photosensitizers: A Novel Approach to Antibacterial Treatment. In *Antibiotic Therapy: New Developments*; 2013; pp 63–88.

(19) Pérez-Laguna, V.; García-Luque, I.; Ballesta, S.; Pérez-Artiaga, L.; Lampaya-Pérez, V.; Samper, S.; Soria-Lozano, P.; Rezusta, A.; Gilaberte, Y. Antimicrobial Photodynamic Activity of Rose Bengal, Alone or in Combination with Gentamicin, against Planktonic and Biofilm Staphylococcus Aureus. *Photodiagnosis Photodyn. Ther.* **2018**, *21* (October 2017), 211–216.

(20) Huang, L.; Wang, M.; Huang, Y.-Y.; El-Hussein, A.; Wolf, L. M.; Chiang, L. Y.; Hamblin, M. R. Progressive Cationic Functionalization of Chlorin Derivatives for Antimicrobial Photodynamic Inactivation and Related Vancomycin Conjugates. *Photochem. Photobiol. Sci.* **2018**, *17* (5), 638–651.

(21) Dosselli, R.; Tampieri, C.; Ruiz-González, R.; De Munari, S.; Ragàs, X.; Sánchez-García, D.; Agut, M.; Nonell, S.; Reddi, E.; Gobbo, M. Synthesis, Characterization, and Photoinduced Antibacterial Activity of Porphyrin-Type Photosensitizers Conjugated to the Antimicrobial Peptide Apidaecin 1b. *J. Med. Chem.* **2013**, *56* (3), 1052–1063.

(22) Dosselli, R.; Ruiz-González, R.; Moret, F.; Agnolon, V.; Compagnin, C.; Mognato, M.; Sella, V.; Agut, M.; Nonell, S.; Gobbo, M.; et al. Synthesis, Spectroscopic, and Photophysical Characterization and Photosensitizing Activity toward Prokaryotic and Eukaryotic Cells of Porphyrin-Magainin and -Buforin Conjugates. *J. Med. Chem.* **2014**, *57* (4), 1403–1415.

(23) Davies, J.; Wright, G. D. Bacterial Resistance to Aminoglycoside Antibiotics. *Trends Microbiol.* **1997**, *5* (6), 234–

240.

(24) Hayward, R. S.; Harding, J.; Molloy, R.; Land, L.; Longcroft-Neal, K.; Moore, D.; Ross, J. D. C. Adverse Effects of a Single Dose of Gentamicin in Adults: A Systematic Review. *Br. J. Clin. Pharmacol.* **2018**, *84* (2), 223–238.

(25) Hamblin, M. R. Antimicrobial Photodynamic Inactivation: A Bright New Technique to Kill Resistant Microbes. *Curr. Opin. Microbiol.* **2016**, *33*, 67–73.

(26) Vogel, E.; Richert, C.; Benninghaurs, T.; Müller, M.; D. Cross, A. Porphycene Compounds for Photodynamic Therapy. *US Pat. 5,409,900* **1993**.

(27) Setsune, J. 2,2′-Bipyrrole-Based Porphyrinoids. *Chem. Rev.* **2017**, *117* (4), 3044–3101.

(28) Anguera, G.; Sánchez-García, D. Porphycenes and Related Isomers: Synthetic Aspects. *Chem. Rev.* **2017**, *117* (4), 2481–2516.

(29) Sanchez-Garcia, D.; Borrell, J. I.; Nonell, S. One-Pot Synthesis of Substituted 2,2 '-Bipyrroles. A Straightforward Route to Aryl Porphycenes. *Org. Lett.* **2009**, *11* (1), 77–79.

(30) Frigerio, M.; Santagostino, M.; Sputore, S. A User-Friendly Entry to 2-Iodoxybenzoic Acid (IBX). *J. Org. Chem.* **1999**, *64* (12), 4537–4538.

(31) Jurić, S.; Kronja, O. Reactivity of Some Tertiary Chlorides with Olefinic and Methoxy Neighboring Groups. A Case of Extended π, n-Participation. *J. Phys. Org. Chem.* **2002**, *15* (8), 556–560.

(32) Ikeda, H.; Sessler, J. L. Synthesis of the First α-Linked Quaterpyrrole. *J. Org. Chem.* **1993**, *58* (8), 2340–2342.

(33) Planas, O.; Gallavardin, T.; Nonell, S. A Novel Fluoro-Chromogenic Click Reaction for the Labelling of Proteins and Nanoparticles with near-IR Theranostic Agents. *Chem. Commun.* **2015**, *51* (26), 5586–5589.

(34) Planas, O.; Fernández-Llaneza, D.; Nieves, I.; Ruiz-Gonzalez, R.; Lemp, E.; Zanocco, A. L.; Nonell, S. Acid- and Hydrogen-Bonding-Induced Switching between 22-π and 18-π Electron Conjugations in 2-Aminothiazolo[4,5-c]Porphycenes. *Phys. Chem. Chem. Phys.* **2017**, *19* (37), 25537–25543.

(35) Vogel, E.; Mueller, M.; Halpern, O.; D. Cross, A. 9-Substituted Porphycenes. US5610175, 1998.

(36) Sandoval, R.; Leiser, J.; Molitoris, B. A. Aminoglycoside Antibiotics Traffic to the Golgi Complex in LLC-PK1 Cells. *J. Am. Soc. Nephrol.* **1998**, *9* (2), 167–174.

(37) Woiwode, U.; Sievers-Engler, A.; Lämmerhofer, M. Preparation of Fluorescent Labeled Gentamicin as Biological Tracer and Its Characterization by Liquid Chromatography and High Resolution Mass Spectrometry. *J. Pharm. Biomed. Anal.* **2016**, *121*, 307–315.

(38) Isoherranen, NinSoback, S. Determination of Gentamicins C1,C1a, and C2 in Plasma and Urine by HPLC. *Clin. Chem.* **2000**, *46* (6), 837–842.

(39) Planas, O.; Gallavardin, T.; Nonell, S. Unusual Properties of Asymmetric Porphycenes. In *Handbook of Porphyrin Science*; Guilard, R., Smith, K. M., Kadish, K. M., Eds.; World Scientific Publishers, 2016; pp 299–349.

(40) Jori, G. Far-Red-Absorbing Photosensitizers: Their Use in the Photodynamic Therapy of Tumours. *J. Photochem. Photobiol. A Chem.* **1992**, *62* (3), 371–378.

(41) Seybold, P. G.; Gouterman, M. Porphyrins XIII: Fluorescence Spectra and Quantum Yields. *J. Mol. Spectrosc.* **1969**, *31*, 1–13.

(42) Schmidt, R.; Tanielian, C.; Dunsbach, R.; Wolff, C.; Womb, C. Phenalenone, a Universal Reference Compound for the Determination of Quantum Yields of Singlet Oxygen Sensitization. *J. Photochem. Photobiol. A Chem.* **1994**, *79* (1–2), 11–17.

(43) Nonell, S.; González, M.; Trull, F. R. 1H-Phenalen-1-One-2-Sulfonic Acid: An Extremely Efficient Singlet Molecular Oxygen Sensitizer for Aqueous Media. *Afinidad* **1993**, *44*, 445–450.

(44) Prat, F.; Stackow, R.; Bernstein, R.; Qian, W.; Rubin, Y.; Foote, C. S. Triplet-State Properties and Singlet Oxygen Generation in a Homologous Series of Functionalized Fullerene Derivatives. *J. Phys. Chem. A* **1999**, *103* (36), 7230–7235.

(45) Jiang, X.-J.; Yeung, S.-L.; Lo, P.-C.; Fong, W.-P.; Ng, D. K. P. Phthalocyanine-Polyamine Conjugates as Highly Efficient Photosensitizers for Photodynamic Therapy. *J. Med. Chem.* **2011**, *54* (1), 320–330.

(46) Lin, D.; Wang, Y.; Zhang, Q.; Zhou, J.; Zhou, L.; Wei, S. The Substituted Amino Group Type Dependent Sensitivity Enhancing of Cationic Phthalocyanine Derivatives for Photodynamic Activity. *J. Photochem. Photobiol. A Chem.* **2016**, *315*, 107–120.

(47) Jakobsen, L.; Sandvang, D.; Jensen, V. F.; Seyfarth, A. M.; Frimodt-Møller, N.; Hammerum, A. M. Gentamicin Susceptibility in Escherichia coli Related to the Genetic Background: Problems with Breakpoints *Clin. Microbiol. Infect*. **2007,** *13* (8), 830-832.

(48) Barra, F.; Roscetto, E.; Soriano, A.; Vollaro, A.; Postiglione, I.; Pierantoni, M.; Palumbo, G.; Catania, M. Photodynamic and Antibiotic Therapy in Combination to Fight Biofilms and Resistant Surface Bacterial Infections. *Int. J. Mol. Sci.* **2015**, *16* (9), 20417–20430.

(49) Pérez-Laguna, V.; García-Luque, I.; Ballesta, S.; Pérez-Artiaga, L.; Lampaya-Pérez, V.; Samper, S.; Soria-Lozano, P.; Rezusta, A.; Gilaberte, Y. Antimicrobial Photodynamic Activity of Rose Bengal, Alone or in Combination with Gentamicin, against Planktonic and Biofilm Staphylococcus Aureus. *Photodiagnosis Photodyn. Ther.* **2018**, *21*, 211–216.

(50) Dosselli, R.; Gobbo, M.; Bolognini, E.; Campestrini, S.; Reddi, E. Porphyrin−Apidaecin Conjugate as a New Broad Spectrum Antibacterial Agent. *ACS Med. Chem. Lett.* **2010**, *1* (1), 35–38.

(51) Le Guern, F.; Ouk, T.-S.; Ouk, C.; Vanderesse, R.; Champavier, Y.; Pinault, E.; Sol, V. Lysine Analogue of Polymyxin B as a Significant Opportunity for Photodynamic Antimicrobial Chemotherapy. *ACS Med. Chem. Lett.* **2018**, *9* (1), 11–16.

(52) Cahan, R.; Swissa, N.; Gellerman, G.; Nitzan, Y. Photosensitizer-Antibiotic Conjugates: A Novel Class of Antibacterial Molecules. *Photochem. Photobiol.* **2010**, *86* (2), 418–425.

(53) Smith, C. R. Activated Zinc Dust. *Synlett* **2009**, No. 9, 1522–1523.

(54) Chen, J.; Du, X. Novel Synthetic Routes of 3-Methoxypropanal from Glycerol. *Synth. Commun.* **2011**, *41*, 1376–

1380.

(55) Chen, C.-Y.; Hart, D. J. A Diels-Alder Approach to Stemona Alkaloids: Total Synthesis of Stenine. *J. Org. Chem.* **1993**, *58* (11), 3840–3849.

(56) Richert, C.; Wessels, J. M.; Mueller, M.; Kisters, M.; Benninghaus, T.; Goetz, A. E. Photodynamic Antitumor Agents: .Beta.-Methoxyethyl Groups Give Access to Functionalized Porphycenes and Enhance Cellular Uptake and Activity. *J. Med. Chem.* **1994**, *37* (17), 2797–2807.

(57) Jiménez-Banzo, A.; Ragàs, X.; Kapusta, P.; Nonell, S. Time-Resolved Methods in Biophysics. 7. Photon Counting vs. Analog Time-Resolved Singlet Oxygen Phosphorescence Detection. *Photochem. Photobiol. Sci.* **2008**, *7* (9), 1003–1010.